KUO-HSI CHENG. The Influence of Environmental Tobacco Smoke on the Lifetime Probability of Lung Cancer due to Exposure to Radon (Under the direction of Douglas J. Crawford-Brown)

ABSTRACT

An analysis concerning the effect of environmental tobacco smoke (ETS) on estimation of lifetime risk of radon-induced lung cancer is made. Based on the consideration of radon dosimetry as a function of age, a generalized state-vector model is used to estimate the total probability of lung cancer due to exposure to both radon and ETS during a normal (73 year) lifespan. This report suggests that there is a general tendency of increasing working level concentration of radon progeny and decreasing unattached fraction of radon progeny RaA (Po-218) with greater amounts of ETS present in the home. The initial concentration of ambient aerosols plays an important role in quantifying the effect of ETS on radon exposure. The combined ETS and radon exposure may either raise or lower the risk of lung cancer associated with radon exposure alone, primarily depending upon the initial aerosol concentration and amounts of cigarette smoke.

ACKNOWLEDGEMENT

I would like to extend appreciation to my research advisor, Dr. D. J. Crawford-Brown, for his encouragement, support, guidance throughout the development and completion of this study and during my graduate training. The other members of the advisory committee, Dr. A. G. Turner and Dr. J. E. Watson, are gratefully acknowledged for their review and valuable suggestions in preparation of this report.

I am indebted to Dr. W. Hofmann who generously provided his computer code for calculating the dose of radon progeny. In addition, gratitude is also expressed to my girlfriend, Yi-Hsin Yang, who assisted in computer work of fitting the spline functions and provided the moral and emotional support during the hard time of preparing this report.

This report is especially dedicated to my parents and family in Taiwan.

TABLE OF CONTENTS

LIST OF TABLES

LIST OF FIGURES

LIST OF ABBREVIATIONS

BEIR	Committee on the Biological Effects of Ionizing Radiations
EPA	Environmental Protection Agency
ETS	Environmental Tobacco Smoke
MMAD	Mass Median Aerodynamic Diameter
MS	Mainstream
NCRP	National Council on Radiation Protection and Measurements
NOPL	Naso-oro-pharyngo-laryngeal
NRC	National Research Council
RaA	Progeny Radium A (Po-218)
RaB	Progeny Radium B (Pb-214)
RaC	Progeny Radium C (Bi-214)
RSP	Respirable Suspended Particulates
SS	Sidestream
TB	Tracheobronchial
WL	Working Level
WLM	Working Level Month

I. INTRODUCTION

The health risks related to indoor radon and environmental tobacco smoke (ETS) are of great public concern. The evidence from epidemiological studies of uranium miners and from animal experiments suggests that there is a strong association between exposure to radon and lung cancer (NRC88). However, the relationship between ETS and lung cancer is controversial at the moment. Some studies have concluded that exposure to ETS causes lung cancer, but others found no significant effect. It is noted that many previous studies have been conducted to assess each of these two pollutants associated with lung cancer separately, but little attempt has been made to examine the combined risk from exposure to radon and ETS simultaneously.

The purpose of this study is to estimate the lifetime risk of radon-induced lung cancer by considering the effect of ETS on the tracheobronchial (TB) distribution and dose of radon progeny. In addition, the issue of radon dosimetry as a function of age will be taken into account in calculating the delivered dose to the lung for each age.

Chapter 2 explains the theoretical framework for estimating the lifetime risk of lung cancer attributable to exposure to radon and ETS. This includes the assumptions, mathematical models, and

solutions for estimating exposure conditions, deposition of radon progeny, doses to the lung, and the probability of developing lung cancer.

Chapter 3 discusses the parameter values used in estimating exposure conditions; and, the parameter values used in the state-vector model for estimating the lifetime risk of lung cancer.

Chapter 4 presents the final results, including the effect of ETS on radon progeny working level (WL) concentration and unattached fraction of progeny RaA; the annual doses under each set of exposure conditions for each age; and, the different ratios of risks (with ETS/smoke free) under each set of exposure conditions.

Chapter 5 discusses the implications of the results found in this study, including the relevance to other studies and interpretation for mitigation purposes.

Chapter 6 includes further investigations and recommendations for future research.

1.1. A Brief Review of Radon

Radon is a radioactive gas occurring naturally by alpha decay of radium-226 in rocks and soil. As radon undergoes the radioactive decays , it decomposes into short-lived decay products called radon progeny. Radon progeny are chemically active and believed to contribute a major portion of the biologically significant doses when they deposit in the lung. Indoor airborne radon arises principally from the following sources : the basement floor under which the rocks and soil are located, many building materials, and radon-

containing water supply. Since radium can be found almost everywhere in the earth's crust, all homes actually contain some levels of radon. Due to the ubiquity of radon in homes, there is a growing concern about its associated health risks among the general population.

In the 1988-1989 home surveys in 25 states conducted by the U.S. Environmental Protection Agency (EPA87), homes in many states have a radon concentration exceeding the action level (4 pCi/L) set by the EPA. Among these surveyed states, Iowa (71%), North Dakota (63%), and Minnesota (46%) have the highest percentage. Even though indoor radon concentration varies from home to home, which is basically dependent on house characteristics and geological areas, an annual average radon level of 0.83 pCi/L or 0.004 working level (WL) is used by the EPA for estimating the health risk associated with radon exposure (EPA 87).

There have been a number of investigations of radon-related health risks of underground miners since the United Nations Scientific Committee on the Effects of Atomic Radiation (UNSCEAR) 1977 report was issued (NRC90). Because different models and risk coefficients were used, the risk estimates due to radon exposure vary significantly, ranging from 130 to 730 deaths out of 10^6 persons per working level month (WLM). For example, the Biological Effects of Ionizing Radiations (BEIR) III Committee used a constant absolute risk model which generated the highest estimate of 730 deaths per 10^6 person WLM. The National Council on Radiation Protection and Measurement (NCRP) used an absolute risk model with exponentially decreasing risks with time after exposure and projected a lowest

estimate of 130 deaths per 10^6 person WLM. In contrast, the BEIR IV committee used the time and age dependent relative risk model which resulted in a moderate estimate of 350 attributable lung cancer deaths per 10^6 person WLM. Overall, the lifetime risk of lung cancer due to indoor radon exposure is about 400 per million persons per WLM, and the lifetime exposure dose is approximately 15 WLM (Lao90).

The EPA estimated a radon-exposed lung cancer mortality rate of 5,230 to 20,894 per year in the United States. This implies that a probability of 23 to 92 excess lung cancer deaths for each one million people per year is attributable to indoor radon exposure (Lao90).

1.2. A Brief Review of Environmental Tobacco Smoke

ETS is a complex substance containing over 4,000 chemicals, which primarily comes from a combination of sidestream (SS) smoke released from the burning end of the cigarettes and exhaled mainstream (MS) smoke emitted from the smokers. The SS smoke contributes the major constituents to ETS. Each mixture, SS, MS, and ETS, is an aerosol consisting of a particulate phase and a vapor phase. The concentration of many carcinogenic and other toxic compounds is higher in SS smoke than in MS smoke. Included are ammonia, volatile amines, volatile nitrosamines, nicotine decomposition products, and aromatic amines (NRC86). Many field studies and mathematical models have demonstrated that ETS is one of the major potential sources of indoor air pollutants and contributes a significant portion of particles to indoor air pollution.

The potentially adverse effects of ETS may range from irritation or acute respiratory disease to fatal lung cancer due to regular long-term exposure. Since mainstream smoke is believed to cause lung cancer, the possibly qualitative similarities between ETS and mainstream smoke make it reasonable to suspect that long-term exposure to ETS might increase the risk of developing lung cancer.

The National Research Council (NRC) concluded that epidemiological studies have demonstrated an association between lung cancer in nonsmokers and ETS exposure, and that laboratory experiments provide a biological plausibility for ETS to cause lung cancer in human cells (NRC86). Based on the review and analysis of 24 epidemiological studies, a formal risk assessment done by EPA concluded that ETS is a Group A carcinogen known to cause lung cancer in human (EPA90). However, a number of scientists have suggested that epidemiological studies of ETS are not reliable due to the possibility of recall bias, misclassification, and other methodological problems. The risk assessment of ETS based on these questionable studies can not prove the causality between ETS exposure and increased risk of lung cancer. The difficulty in identifying ETS effects arises primarily for the following three reasons : (1) ETS is a complex mixture containing over 4,000 components whose biological effects can not be precisely quantified given the relatively insensitive techniques available, (2) epidemiology is too blunt a tool to distinguish between "very low risk" and "no risk" of lung cancer from ETS (Roe90), and (3) ETS may interact with numerous other indoor air pollutants, including radon, asbestos, formaldehyde, and others.

II. THEORETICAL FRAMEWORK

To predict the lifetime risk of lung cancer attributable to exposure to radon and ETS, the risk assessment is broken into the following analytical steps : (1) estimation of the exposure conditions for radon with and without ETS present, (2) calculation of the deposition of radon progeny in the tracheobronchial (TB) region of the lung under each set of exposure conditions, (3) calculation of the doses to the epithelial cells in each generation of the lung under each set of exposure conditions, and (4) calculation of the probability of lung cancer from these doses under each set of exposure conditions.

2.1. Estimation of Exposure Conditions:

In this study, the radon concentration in indoor air is assumed to remain at a constant value of 1 pCi/L, which is reported as the approximate average indoor concentration of radon in the U.S. (NCRP84). The indoor progeny derive from the radioactive decay of airborne radon in the home and transport through ventilation from the outside atmosphere. A fraction of the radon progeny exists in a free form called the unattached fraction, while the remainder is attached to aerosol particles. Free progeny with a positive charge will undergo one of the following fates:

(1) They migrate onto room surfaces to which they are attached.

(2) They attach to aerosol particles in the room, and are either inhaled along with the particles, deposited on room surfaces along with the particles, or released from particles into a free form again due to recoil during subsequent decay.

(3) They remain free in air and eventually will be inhaled.

A block diagram depicting the general features of the decay, transport, and attachment of radon progeny is shown in Figure 1.

Several parameters appearing in Figure 1 are defined as follows: (1) λ_i (time^{-1}) is the radioactive decay rate constant for the i^{th} progeny, (2) λ_v (time^{-1}) is the rate of ventilation, (3) $\lambda_{d,f}$ and $\lambda_{d,a}$ (time^{-1}) are the rates of deposition onto room surfaces for free and attached progeny, respectively, (4) α_i is the fraction of the i^{th} attached progeny that release from attachment to aerosol particles during subsequent decay, and, finally, (5) λ_s (time^{-1}) is the rate of attachment of free progeny to aerosol particles.

The relation between λ_s and ambient particle conditions is given in the form of (NRC88):

$$\lambda_s = N \pi d^2 v / 4 \qquad (1)$$

Where: N = concentration of particles in air (cm^{-3})

d = median diameter of particles in air (cm)

v = mean ion velocity in air (cm/sec), employed here to be 1.38×10^4 (Raa69)

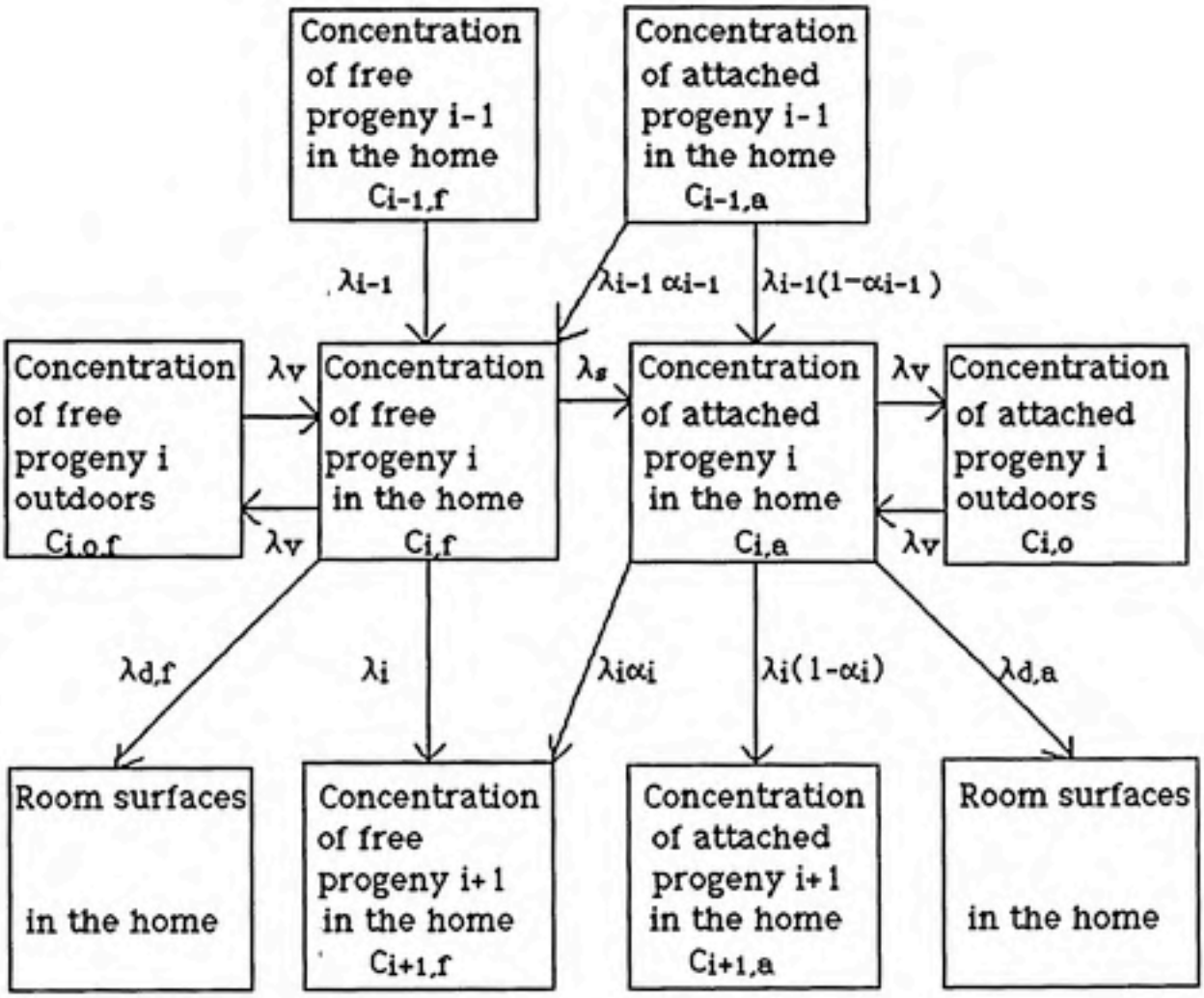

Figure 1 Flow Diagram for Various Fates of Radon Progeny in the Home

From the flow diagram shown in Figure 1, two differential equations in the form of general expressions for the i^{th} progeny may be written to describe the rate of change of concentrations of the progeny which are either free ($C_{i,f}(t)$) in air or attached to aerosol particles ($C_{i,a}(t)$) :

$$\frac{d\,C_{i,f}(t)}{d\,t} = \lambda_{i-1}C_{i-1,f}(t) + \lambda_v C_{i,o,f}(t) + \lambda_{i-1}\alpha_{i-1}C_{i-1,a}(t) - \lambda_{d,f}C_{i,f}(t) - \lambda_v C_{i,f}(t) - \lambda_i C_{i,f}(t) - \lambda_s C_{i,f}(t) \quad (2)$$

$$\frac{d\,C_{i,a}(t)}{d\,t} = \lambda_v C_{i,o,a}(t) + \lambda_s C_{i,f}(t) + \lambda_{i-1}(1 - \alpha_{i-1})C_{i-1,a}(t) - \lambda_{d,a}C_{i,a}(t) - \lambda_i\alpha_i C_{i,a}(t) - \lambda_v C_{i,a}(t) - \lambda_i(1-\alpha i)C_{i,a}(t) \quad (3)$$

Here, the subscript i equal to A represents the progeny RaA (Po-218), i equal to B represents the progeny RaB (Pb-214), and i equal to C represents the progeny RaC (Bi-214); the subscript f denotes the free progeny (unattached to aerosol); the subscript o means the outdoor atmosphere; and, the subscript a stands for the progeny attached to aerosol particles.

In an undisturbed area with little air circulation, the short-lived progeny will come into equilibrium with the parent radon (NCRP85). Upon reaching the state of equilibrium, the progeny concentrations will not change with time. This means that equations (2) and (3) may be solved at equilibrium by setting $dC_{i,f}(t)/dt$ and $dC_{i,a}(t)/dt$ equal to zero. Also it is assumed that the concentrations

of indoor radon (C_{222}) and outdoor progeny ($C_{i,o,f}$ and $C_{i,o,a}$) are constant in time.

At equilibrium, the concentrations of progeny are:

$$C_{A,f} = \frac{\lambda_{222} C_{222} + \lambda_v C_{A,o,f}}{\lambda_{d,f} + \lambda_v + \lambda_A + \lambda_s} \quad (4)$$

$$C_{A,a} = \frac{\lambda_v C_{A,o,a} + \lambda_s C_{A,f}}{\lambda_{d,a} + \lambda_A + \lambda_v} \quad (5)$$

$$C_{B,f} = \frac{\lambda_A C_{A,f} + \lambda_v C_{B,o,f} + \lambda_A \alpha_A C_{A,a}}{\lambda_{d,f} + \lambda_v + \lambda_B + \lambda_s} \quad (6)$$

$$C_{B,a} = \frac{\lambda_v C_{B,o,a} + \lambda_s C_{B,f} + \lambda_A (1-\alpha_A) C_{A,a}}{\lambda_{d,a} + \lambda_B + \lambda_v} \quad (7)$$

$$C_{c,f} = \frac{\lambda_B C_{B,f} + \lambda_v C_{C,o,f} + \lambda_B \alpha_B C_{B,a}}{\lambda_{d,f} + \lambda_v + \lambda_C + \lambda_s} \quad (8)$$

$$C_{c,a} = \frac{\lambda_v C_{c,o,a} + \lambda_s C_{c,f} + \lambda_B (1-\alpha_B) C_{B,a}}{\lambda_{d,a} + \lambda_C + \lambda_v} \quad (9)$$

In equations (4)-(9), the units of the concentrations are atoms per liter of air (atoms/L). From the report of the NCRP (NCRP85), the approximate number of atoms per pCi is 18,000, 10, 85, and 63 for

Rn, RaA, RaB ,and RaC, respectively. Concentrations in pCi/L may be obtained by dividing the results of equations (4)-(9) by the appropriate conversion factor from the NCRP report.

Working level (WL) is the common unit employed in risk analyses for radon progeny, originally in uranium mines but now in environmental exposures as well. Numerically, the WL is any combination of short-lived progeny in one liter of air that will result in the emission of 1.3 x 10^5 MeV of potential alpha energy (NCRP88). It is calculated from the following relation (Ev68):

$$WL = 0.00103\ (C_{A,f} + C_{A,a}) + 0.00507\ (C_{B,f} + C_{B,a}) + 0.00373\ (C_{c,f} + C_{c,a}) \quad (10)$$

In equation (10), all concentrations are expressed in units of pCi/L.

The presence of ETS will influence the concentration of aerosol particles to which the radon progeny may attach. The results of measurements of the mean diameter of particles in SS smoke have been reported in several studies. The mass median aerodynamic diameter (MMAD) for ETS particles was measured by McCusker et al. (Mc83) and ranged from 0.37 to 0.52 μm, which is similar to the results obtained by Keith (Kei60) using a specially modified centrifuge. The aging of ETS will reduce the MMAD by a factor of 2 to 3 due to the loss of larger particles by settling (Kei60, Wy67, In85). Therefore, the MMAD for ETS particles is approximately 0.15 μm, which is consistent with the MMAD for ambient indoor aerosols to which radon progeny normally are attached without the presence of ETS. This implies that the addition of ETS changes the concentration (N) but not the diameter (d) of particles in air in equation (1).

2.2. Calculation of Deposition and Doses

Based on the fact that the observed lung cancers among uranium miners appear to occur primarily in the TB region (Mc80), the basal cells of the bronchial epithelium are regarded as the most radiosensitive and are the target cells for lung cancer induced by radiation from radon progeny. The calculation of deposition probability in the TB region for radon progeny is determined by the breathing rate, the size distribution and the unattached fraction of progeny, and the filtration efficiency of the nasopharyngeal region (Lao90). While several processes contribute to the deposition of aerosol particles in a cylindrical tube like the lung airway, the three most important mechanisms of deposition are impaction, sedimentation, and diffusion. The total probability, P(n), of a particle depositing in the n^{th} generation of the lung is given by (C-B87):

$$P(n) = 1 - [\ 1 - P_I(n)\ ]\ [\ 1 - P_s(n)\ ]\ [1 - P_D(n)\ ] \qquad (11)$$

where, $P_I(n)$, $P_s(n)$, and $P_D(n)$ represent the fractions of particles which deposit by impaction, sedimentation, and diffusion, respectively, in the n^{th} generation.

After calculating total deposition in each generation of the lung for the radon progeny, the radiation dose is estimated by the following steps : (1) mucus flow is modeled to calculate how the progeny move; (2) this movement is used to estimate the site of decay for the progeny, yielding decays/cm^2 in each generation during a year of exposure; (3) depth-dose curves are developed to yield dose per decay/cm^2; and, finally (4) dose to basal cells is

calculated by multiplying the result of (2) and (3). This dose calculation based on the location of critical cells relative to the site of decay for progeny takes into account the shielding effect of mucociliary layer, mucus thickness, bronchial morphometry, and other factors. The detailed processes for modeling movement on the mucociliary blanket, computing areal density of the radon progeny on the walls of the generations, and generating depth-dose curves refer to "Dosimetry" by Crawford-Brown (C-B87).

For purposes of this report, deposition of progeny in the generations of the TB region and dose to basal cells of the lung were calculated using the computer code of Hofmann.

The age-variant doses under each set of exposure conditions are shown in Tables 5 to 8.

2.3. Risk Estimation

The generalized state-vector model of radiation carcinogenesis by Crawford-Brown and Hofmann (C-B90) has been demonstrated to successfully explain patterns found in experimental or epidemiological studies involving radiation and cancer. The concept of this model is that a cell must pass through several distinctive stages to produce a fatal tumor. Unlike the multistage model, the state-vector model specifies the biophysical meaning of each transition and stage in terms of initiation, promotion, and progression.

Initiation is triggered when a cell experiences DNA damage and has undergone a required number of divisions. The whole process of

initiation is characterized by the following four steps : (1) inception of a first specific DNA strand break, (2) occurrence of a second less specific DNA strand break, (3) interaction of the above two breaks, and (4) division-related fixation of this primary damage. Promotion is produced by the loss of contact inhibition in a focus of cells, which for radiation occurs due to the loss of proliferative capacity in a fraction of the cells surrounding an initiated cell (C-B90). Progression is associated with the growth of the promoted cells into a frank tumor. This transition is related to the kinetics of growth, death, and removal of cancer cells.

In the following risk estimation, this model will be used to calculate the lifetime probability of lung cancer. The lifetime risk of lung cancer is assumed to be proportional to the number of cells reaching the state of progression during a normal (73 year) lifespan.

2.3.1. Description of State-Vector Model

The model is designed to describe radiation induced cellular transformation by assuming that an initially undamaged cell must pass through 7 states (from state 0 to state 6) to yield a colony of transformed cells, especially for alpha irradiation due to radon exposure. The features of the model may be found in figure 2 and the details are discussed below.

State 0 refers to cells in a normal and undamaged state. Cells in state 0 have not yet experienced any lesion after exposure to radiation or chemicals starts.

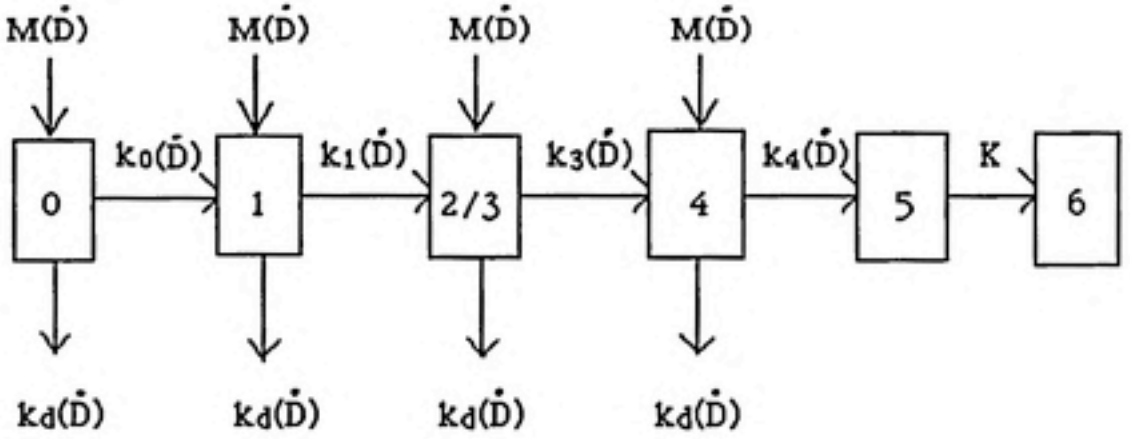

Where: Numerical number i (i.e. from 0 to 6) represents state i
$M(\dot{D})$ is the rate of mitosis (day^{-1})
$k_d(\dot{D})$ is the rate of cell killing (day^{-1})
$k_i(\dot{D})$ is the rate of transition for state i (day^{-1})
K is the fraction of cells in state 5 moved to state 6

Figure 2 State - vector Model

State 1 is reached when a cell has experienced a specific DNA strand break. The transition from states 0 to 1 is assumed to be characterized by first-order kinetics with a rate constant $k_0(\dot{D})$, which is a function of the dose rate $\dot{D}$ during each year of exposure. It is important to bear in mind here and in the remaining discussion that $\dot{D}$ will vary with age due to changes in breathing characteristics and lung anatomy.

A cell reaches state 2 when it suffers a second less specific DNA double strand break(C-B90). This transition governed by first-order kinetics with a rate constant $k_1(\dot{D})$ is also a function of dose rate $\dot{D}$.

State 3 represents an interaction between the first and the second DNA double-stranded breaks, which for alpha irradiation occurs immediately after a cell has reached state 2.

The transition to state 4 is the result of cell division. During each division, only a required fraction (P_4) of cells in state 3 are moved into state 4 (C-B90). This transition is referred to as division-related fixation of primary lesions, with a rate constant $k_3(\dot{D})$ which is dependent on the rate of mitosis of cells in state 3. This rate of mitosis is related to $\dot{D}$ due to stimulation of cell division by cytotoxicity.

The transition of a cell to state 5 is the result of promotion. As discussed earlier, the rate of promotion $k_4(\dot{D})$ contains a spontaneous rate and a radiation induced component. This radiation-induced transition occurs when a required fraction of the cells surrounding a state 4 cell loses proliferative capacity. From histological considerations, an epithelial cell is found to be surrounded by six other contiguous cells. Radiation induced promotion occurs when

four out of these six neighboring cells are killed (C-B90). The loss of proliferative ability of dead cells interrupts cellular inter-communication within the community to yield an uncontrolled growth of cells in state 5. This is referred to as contact inhibition removal.

A cell in state 6, the final state, has progressed from a preneoplastic lesion to a frank tumor. The study of atomic bomb survivors suggests that the latency period of cancer is not significantly affected by radiation (Shi90). Based on this information, it is assumed here that a fraction K of state 5 cells are moved to state 6, and that K is not a function of $\dot{D}$. This implies that any cell reaching state 5 has an equal chance to produce cancer regardless of time or dose rate.

Prior to state 5, there are rate constants for cell killing, $K_d(\dot{D})$, and for the mitosis of cells, $M(\dot{D})$, in each state, respectively. These two transition rates are assumed to include a spontaneous rate, which is based on the belief that a natural transition would occur without any delivered dose, and a radiation induced rate, which is considered to be governed by linear kinetics (details discussed in the next chapter). In addition, the spontaneous rate of mitosis is an age-dependent parameter due to organ growth prior to adulthood. Both spontaneous rates, therefore, change with age.

To complete the final risk estimation, the interaction of ETS and radon progeny must be taken into account. A multiplicative model is used to depict the mechanism of interaction (NRC88). This model assumes that ETS acts as a promoter in the process of carcinogenesis induced by radon progeny. This relationship is given in the form of:

$$RR = RR_{radon} (1 + 0.024\ n) \qquad (12)$$

where RR is the final estimate of relative risk of lung cancer, RR_{radon} is the relative risk from radiation alone, and n is the rate of cigarettes smoked (in units of packs per day). Given a recent report from experimental data (Gri88), the particulate phase of cigarette smoke is considered to contain the primary carcinogens for most induced cancers. It is assumed that the mass of respirable suspended particulates (RSP) deposited in the TB region is an appropriate measurement of carcinogenicity for both MS smoke and ETS. Therefore, the conversion from exposure to MS smoke to exposure to ETS is based on the assumption that the total deposition of RSP in the TB airways is an approximate measure of equivalence (NRC86). The total inhaled mass of RSP has been calculated by Wells (We88) to be 240 mg for the active smoker and 3 mg for the passive smoker. Multiplying these values by the TB deposition fractions (C-B82) yields 36 mg of total deposited RSP for the active smoker and 0.12 mg of total deposited RSP for the passive smoker. If an active smoker consumes one pack of cigarettes per day in the home, the passive smoker would inhale a mass of RSP equivalent to 0.08 cigarettes per day. Multiplying this quantity by the excess risk of smoking miners (i.e. 0.3) yields a value of 0.024. This implies that there is an increased risk of 2.4% in the presence of ETS equal to one pack of cigarettes per day when the promoting effect of ETS is considered in the radon-induced carcinogenesis.

2.3.2. Mathematical Formulations

The quantitative characterization of state-vector model is simply based on the concept that the rate of change of each state is equal to total rate in minus total rate out. Let $N_i(t)$ be the number of cells of the lung in state i at time t after exposure to radon starts. In Figure 2, each box prior to state 5 has a mitotic rate constant $M(\dot{D})$ feeding in and a rate constant of cell killing $k_d(\dot{D})$ flowing out. The product of $N_i(t)$ and $M(\dot{D})$ means the rate of cell increase derived from cell division, while the value of $N_i(t)$ times $k_d(t)$ represents the rate of cell loss due to cell killing. Because of the prompt interaction between states 2 and 3 for alpha irradiation, this should not be considered as a distinctive transition. A single box representing both state 2 and state 3 is used in the state-vector model for the present study.

Based on the above discussion, the differential equations describing this model are:

$$\frac{dN_0(t)}{dt} = M(\dot{D})\, N_0(t) - (k_d(\dot{D}) + k_0(\dot{D}))\, N_0(t) \qquad (13)$$

$$\frac{dN_1(t)}{dt} = k_0(\dot{D})\, N_0(t) + (M(\dot{D}) - k_1(\dot{D}) - k_d(\dot{D}))\, N_1(t) \qquad (14)$$

$$\frac{dN_3(t)}{dt} = k_1(\dot{D})\, N_1(t) + (M(\dot{D}) - k_3(\dot{D}) - k_d(\dot{D}))\, N_3(t) \qquad (15)$$

$$\frac{dN_4(t)}{dt} = k_3(\dot{D})\, N_3(t) + (M(\dot{D}) - k_3(\dot{D}) - k_d(\dot{D}))\, N_4(t) \qquad (16)$$

State 5 is given separately by integral equation due to the constant K independent of dose rate. This means that cells reaching state 5 will pile up and undergo the transition to state 6 with a fixed fraction K.

$$N_5(t) = \int_0^T k_4(\dot{D})\, N_4(t)\, dt \qquad (17)$$

$$\text{But, } N_6(t) = K\, N_5(t) \qquad (18)$$

$$N_6(t) = K \int_0^T k_4(\dot{D})\, N_4(t)\, dt \qquad (19)$$

Therefore, the total probability of lung cancer is:

$$P_c(\dot{D},t) = \int_0^T K\, k_4(\dot{D})\, N_4(t)\, dt \qquad (20)$$

2.3.3. Equation Solutions

Through repetitive applications of Bernoulli's solution (Kel60), the above differential equations are solved as follows:

$$N_0(t) = N_0(0)\, e^{-(k_d(\dot{D}) + k_0(\dot{D}) - M(\dot{D}))\, t} \qquad (21)$$

$$N_1(t) = \frac{k_0(\dot{D})N_0(0)}{B - A}\left(e^{-At} - e^{-Bt}\right) + N_1(0)\, e^{-Bt} \qquad (22)$$

$$N_3(t) = \frac{k_1(\dot{D})k_0(\dot{D})N_0(0)}{B - A}\left(\frac{e^{-At} - e^{-Ct}}{C - A} - \frac{e^{-Bt} - e^{-Ct}}{C - B}\right)$$

$$+ \frac{k_1(\dot{D})N_1(0)}{C - B}\left(e^{-Bt} - e^{-Ct}\right) + N_3(0)\, e^{-Ct} \qquad (23)$$

$$N_4(t) = \frac{k_3(\dot{D})\, k_1(\dot{D})\, k_0(\dot{D})\, N_0(0)}{(B - A)(C - A)}\left(\frac{e^{-At} - e^{-Dt}}{D - A} - \frac{e^{-Ct} - e^{-Dt}}{D - C}\right)$$

$$- \frac{k_3(\dot{D})\, k_1(\dot{D})\, k_0(\dot{D})\, N_0(0)}{(B - A)(C - B)}\left(\frac{e^{-At} - e^{-Dt}}{D - B} - \frac{e^{-Ct} - e^{-Dt}}{D - C}\right)$$

$$+ \frac{k_3(\dot{D})\, k_1(\dot{D})\, N_1(0)}{C - B}\left(\frac{e^{-Bt} - e^{-Dt}}{D - B} - \frac{e^{-Ct} - e^{-Dt}}{D - C}\right)$$

$$+\frac{k_3(\dot{D})N_3(0)}{D-C}\left(e^{-Ct}-e^{-Dt}\right)+N_4(0)\,e^{-Dt} \qquad (24)$$

$$N_5(t)=\frac{k_4(\dot{D})\,k_3(\dot{D})\,k_1(\dot{D})\,k_0(\dot{D})\,N_0(0)}{(B-A)(C-A)}\left[\frac{1}{D-A}\left(\frac{e^{-Dt}-1}{D}-\frac{e^{-At}-1}{A}\right)\right.$$

$$\left.-\frac{1}{D-C}\left(\frac{e^{-Dt}-1}{D}-\frac{e^{-Ct}-1}{C}\right)\right]$$

$$-\frac{k_4(\dot{D})\,k_3(\dot{D})\,k_1(\dot{D})\,k_0(\dot{D})\,N_0(0)}{(B-A)(C-B)}\left[\frac{1}{D-B}\left(\frac{e^{-Dt}-1}{D}-\frac{e^{-Bt}-1}{B}\right)\right.$$

$$\left.-\frac{1}{D-C}\left(\frac{e^{-Dt}-1}{D}-\frac{e^{-Ct}-1}{C}\right)\right]$$

$$+\frac{k_4(\dot{D})\,k_3(\dot{D})\,k_1(\dot{D})\,N_1(0)}{C-B}\left[\frac{1}{D-B}\left(\frac{e^{-Dt}-1}{D}-\frac{e^{-Bt}-1}{B}\right)\right.$$

$$\left.-\frac{1}{D-C}\left(\frac{e^{-Dt}-1}{D}-\frac{e^{-Ct}-1}{C}\right)\right]$$

$$+\frac{k_4(\dot{D})\,k_3(\dot{D})\,N_3(0)}{D-C}\left(\frac{e^{-Dt}-1}{D}-\frac{e^{-Ct}-1}{C}\right)$$

$$- \frac{k_4(\dot{D})\, N_4(0)}{D} \left(e^{-Dt} - 1 \right) + N_5(0) \qquad (25)$$

Where:

$$A = k_d(\dot{D}) + k_0(\dot{D}) - M(\dot{D})$$

$$B = k_d(\dot{D}) + k_1(\dot{D}) - M(\dot{D})$$

$$C = k_d(\dot{D}) + k_3(\dot{D}) - M(\dot{D})$$

$$D = k_d(\dot{D}) + k_4(\dot{D}) - M(\dot{D})$$

As discussed earlier, it is assumed that the lifetime probability of lung cancer is proportional to the number of cells reaching the state of progression (i.e. state 6) during a normal 73-year exposure. Meanwhile, any cell reaching state 5 will undergo the transition to state 6 with a constant fraction regardless of age. Based on the assumption of a 20-year latency period for developing lung cancer, the number of cells reaching state 5 after a 53-year exposure (i.e. $N_5(53)$) can be a measuring scale proportional to the lifetime risk of lung cancer.

To calculate the accumulative probability of lung cancer, the method of dividing the lifetime into intervals assumes a constant annual dose during each year. This means that those dose-dependent parameter values appearing in equations (21) to (25) are constant within a given year. The annual doses are interpolated

using the spline functions to fit a smooth curve among the given data shown in Tables 5 to 8. The detailed discussion refers to Appendix.

The initial condition for calculating the number of cells reaching each state at age 1 is obtained by arbitrarily setting one cell in state 0 at age 0. Inserting $N_0(0) = 1$, $N_1(0) = N_3(0) = N_4(0) = N_5(0) = 0$, and the corresponding parameter values into equations (21) to (25) yields the number of cells in each state at age 1. This obtained vector at age 1 in turn provides the initial condition for calculating the number of cells reaching each state at age 2. Repeating the same computing process, the number of cells reaching state 5 at age 53 can be calculated under each set of exposure conditions using computer software . The relative risks shown in Table 9 are the results of dividing the number of cells in state 5 with different amounts of ETS present by that with smoke free for differing initial aerosol concentrations.

III. DETERMINATION OF PARAMETER VALUES

3.1. Parameters in Estimation of Exposure Conditions

The values of various parameters appearing in equations 4 to 9 must to be determined to estimate the exposure conditions.

Assuming a rate of one entire air circulation per hour for typical home conditions, a value of 0.0167 min^{-1} for the ventilation rate is assumed here. The decay rate constants for Rn, RaA, RaB, and RaC are 1.26 x 10^{-4}, 0.227, 0.026, and 0.035 min^{-1}(NCRP88), respectively. The value of 0.2 min^{-1} for $\lambda_{d,f}$ is the average of values determined by Rudnick and Maher (Ru86) and the NCRP (NCRP84), while the value of 0.0167 min^{-1} for $\lambda_{d,a}$ is adopted from the NCRP (NCRP84) and is applicable to the deposition of cigarette smoke. The fraction of decay for attached RaA that results in unattached RaB, α_A, is approximately equal to 1/2, but for attached RaB (α_B) or attached RaC (α_C) is zero (Raa69). Since the MMAD for both natural aerosols and tobacco smoke particles is approximately identical, the value of 0.15 μm for d is used in equation (1).

In solving for λs, the aerosol density (N), which is affected by the presence of tobacco smoke must be specified. From the report of the NRC (NRC86), a consumption of 1 pack of cigarettes per day will

produce 26 mg of RSP per hour. For a typical home volume of 400 m^3 with ventilation rate equal to 1 hr^{-1}, this rate of release will add an increased aerosol content of 60 $\mu g/m^3$. This amount is equivalent to an increased aerosol density of approximately 2×10^5 cm^{-3} and must be added to the initial particle concentration without ETS present. The same reasoning is applied to smoking rates of 1/2 and 2 packs of cigarettes per day. Therefore, an increased amount equal to 1×10^5 and 4×10^5 cm^{-3} must be added to the initial aerosol concentration for 1/2 and 2 packs of cigarettes per day, respectively.

Table1 provides a detailed list of the values of various parameters for exposure assessment in this study.

3.2. Parameters in State-Vector Model

The values of parameters employed in the state-vector model are assumed to contain a spontaneous rate and a radiation-induced component. This yields the following mathematical formulations:

$$M(\dot{D}) = M_S + M_R(\dot{D}) \quad (26)$$

$$k_d(\dot{D}) = k_{ds} + k_{dR}\,\dot{D} \quad (27)$$

$$k_0(\dot{D}) = k_{0s} + k_{0R}\,\dot{D} \quad (28)$$

$$k_1(\dot{D}) = k_{1s} + k_{1R}\,\dot{D} \quad (29)$$

$$k_3(\dot{D}) = M(\dot{D})\,P_4 \quad (30)$$

$$k_4(\dot{D}) = k_{4s} + k_{4R}(\dot{D}) \quad (31)$$

Here, subscript s refers to the spontaneous component and subscript R denotes the radiation-induced component in each of the above equations.

Table 1 Summary of Parameter Values Employed for Estimation of Exposure Conditions

PARAMETER	VALUE		
λ_v	0.0167		min^{-1}
λ_{222}	1.26×10^{-4}		min^{-1}
λ_A	0.227		min^{-1}
λ_B	0.02		min^{-1}
λ_C	0.035		min^{-1}
$\lambda_{d,f}$	0.2		min^{-1}
$\lambda_{d,a}$	0.0167		min^{-1}
α_A	0.5		
α_B	0		
α_C	0		
d	1.5×10^{-5}		cm
C_{222}	1	pCi/L	(18,000 atoms/L)
$C_{A,f,o}$	0.01	pCi/L	(0.1 atoms/L)
$C_{A,a,o}$	0.09	pCi/L	(0.9 atoms/L)
$C_{B,f,o}$	0.005	pCi/L	(0.425 atoms/L)
$C_{B,a,o}$	0.05	pCi/L	(4.25 atoms/L)
$C_{c,f,o}$	0.002	pCi/L	(0.126 atoms/L)
$C_{c,a,o}$	0.03	pCi/L	(1.89 atoms/L)

3.2.1. Background Transition Rates:

In the case of a natural transition, cell repair from state 1 back to state 0 occurs. This background rate of repair, 0.13 hr^{-1}, is independent of dose rate (discussed later) and taken from in-vitro studies (Roo90). The block diagram for background transition prior to state 4 is depicted in figure 3.

The rate constants for background transition (k_{0s}, k_{1s}, k_{3s}) are determined by the equilibrium values of $N_0(t)$, $N_1(t)$, and $N_3(t)$ without exposure to radon progeny at t equal to 0. These equilibrium values (N_{0E}, N_{1E}, and N_{3E}) calculated by Crawford-Brown and Hofmann using in-vitro data are equal to 0.94, 0.06, 0.001, respectively (C-B90).

a). Spontaneous Rate of Mitosis (M_S):

The process of spontaneous mitosis in the lung occurs mainly in the basal cells of each generation. The dividing basal cells may either be lost by sloughing, or differentiate into epithelial cells, which in turn may be lost by sloughing. The schematic model describing the spontaneous mitosis of the lung is displayed in Figure 4.

The mathematical formulations are given as follows:

$$\frac{d\,N_B(t)}{d\,t} = M_S\,N_B(t) - (\lambda_D + S_B)\,N_B(t) \qquad (32)$$

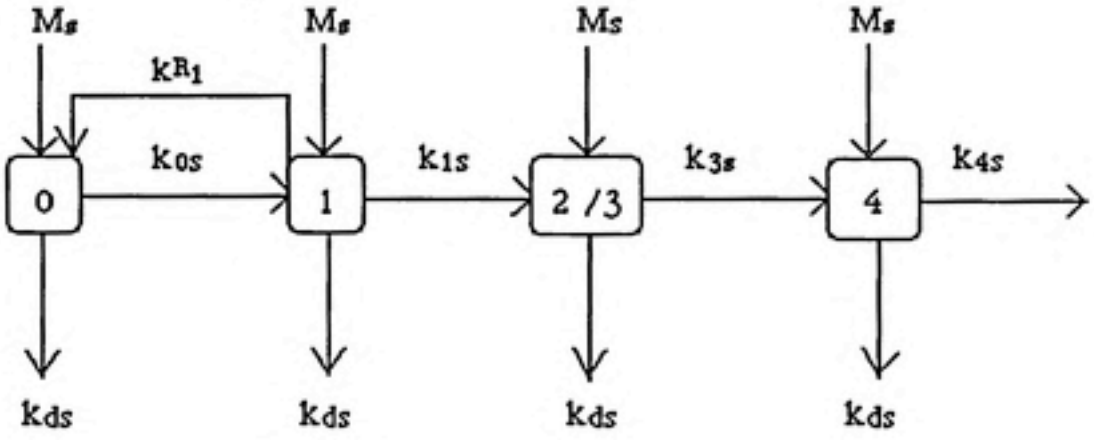

Where: Numerical number i (i.e. o, 1, 2, 3, 4) represents state i
M_s is the spontaneous rate of mitosis (day^{-1})
k_{ds} is the spontaneous rate of cell killing (day^{-1})
k^{R_1} is the rate of cell repair from state 1 back to state 0 (day^{-1})
K_{is} is the spontaneous rate of transition for state i (day^{-1})

Figure 3 Model for Background Transition

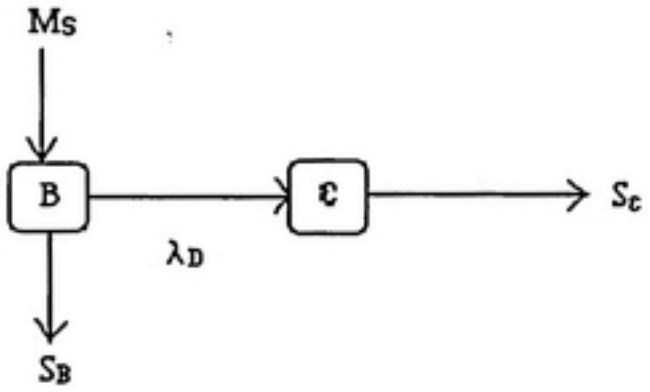

Where: B denotes basal cells

c denotes epithelial cells

M_S is the spontaneous rate of mitosis (day^{-1})

S_B is the rate of sloughing for basal cells (day^{-1})

λ_D is the rate of differentiation (day^{-1})

S_c is the rate of sloughing for epithelial cells (day^{-1})

Figure 4 Model for Spontaneous Mitosis

$$\frac{d\,N_\varepsilon(t)}{d\,t} = \lambda_D\,N_B(t) - S_\varepsilon\,N_\varepsilon(t) \qquad (33)$$

Assume that $N_\varepsilon = k\,N_B$, which means each dividing basal cell could differentiate into k epithelial cells. Inserting this relation into equation (33), M_S is solved as :

$$M_S = \lambda_D\,(1 + 1/k) + S_B - S_\varepsilon \qquad (34)$$

If k equals 1, then

$$M_S = 2\,\lambda_D + S_B - S_\varepsilon$$

Inserting $\lambda_D = (\,M_S + S_\varepsilon - S_B\,)/2$ into equation (32) yields:

$$M_S = 2\,(\frac{1}{N_B}\,\frac{dN_B}{dt}) + (S_B + S_\varepsilon) \qquad (35)$$

If k equals 2, then

$$M_S = 2\,\lambda_D/3 + S_B - S_\varepsilon$$

Inserting $\lambda_D = 2\,(\,M_S + S_\varepsilon - S_B\,)/3$ into equation (32) yields:

$$M_S = 3\,(\frac{1}{N_B}\,\frac{dN_B}{dt}) + (S_B + S_\varepsilon) \qquad (36)$$

A general expression of M_S is :

$$M_S = (k+1)\,(\frac{1}{N}\,\frac{dN}{dt}) + S \qquad (37)$$

Where: $\frac{1}{N}\,\frac{dN}{dt}$ is the fractional rate of change of the lung mass

S equals $(S_B + kS_\varepsilon)$, which is the overall rate of sloughing of lung cells

The value of 2 for k is employed in this study, since there are approximately two epithelial cells for each basal cell in the upper generations of the TB region. Therefore,

$$M_S = 3\left(\frac{1}{N}\frac{dN}{dt}\right) + S \qquad (38)$$

The age dependent values of (1/N) (dN/dt) are shown in Figure 5, taken from a paper by Crawford-Brown (C-B83).

It should be noted that the curve for the whole body is used here due to the absence of data specific to lung epithelium. The age-dependent values of S are determined by the biological half-life in humans of ^{137}Cs in the whole body. It is assumed that ^{137}Cs is retained in the body by attachment to biomolecules in cells. When cells are removed, the contained ^{137}Cs goes with them. Based on this assumption, the half-life of the ^{137}Cs in human bodies is considered to be identical to the half-life for removal of cells. If the mechanism of excretion is governed by a first-order kinetics, the relation of the half life ($T_{1/2}$) and the rate of sloughing (S) is given by:

$$S = 0.693 \,/\, T_{1/2} \qquad (39)$$

The value of $T_{1/2}$ as a function of organ mass (fraction of adult mass) may be seen from Figure 6 (C-B83). The age dependence of organ masses in units of percent of adult value for the human may be found in Figure 7 (C-B83). Therefore, inserting the data from Figure 6 and Figure 7 into equation (39), the age-dependent rates of sloughing (S) can be obtained.

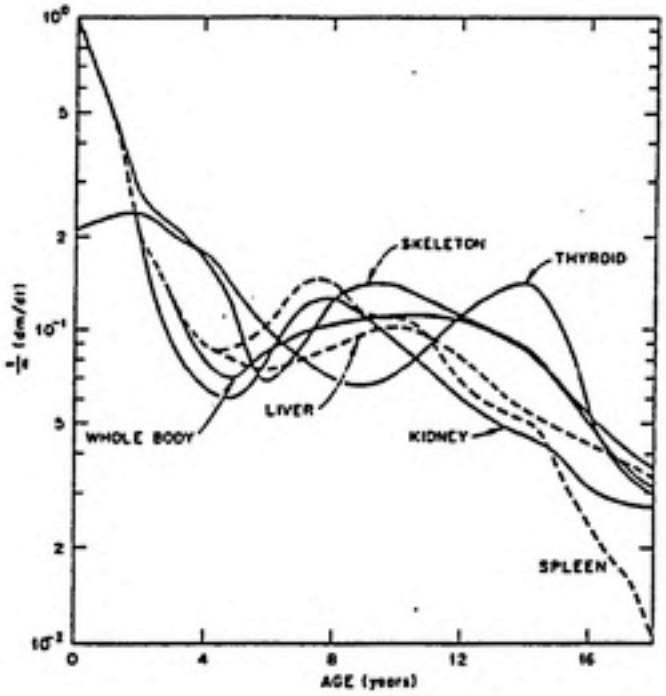

Figure 5 Age Dependence for Fractional Rate of Change of the Organ Masses (yr^{-1}) for the Human

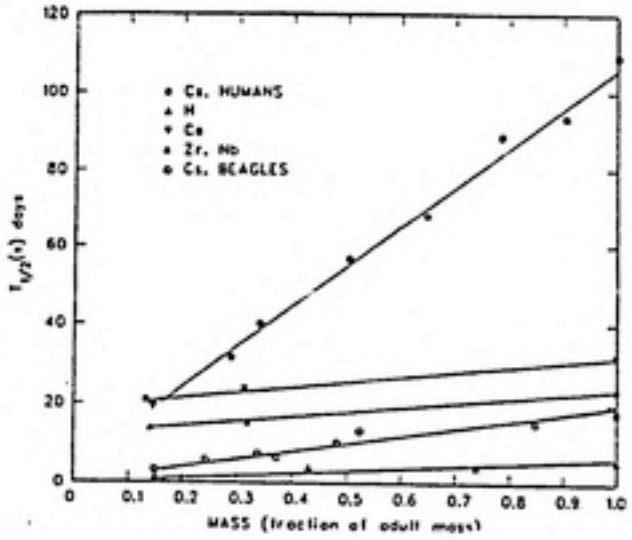

Figure 6 Partial Summary of the Data Used to Develop a Relationship between the Mass and the Biological Half-time in the Whole Body

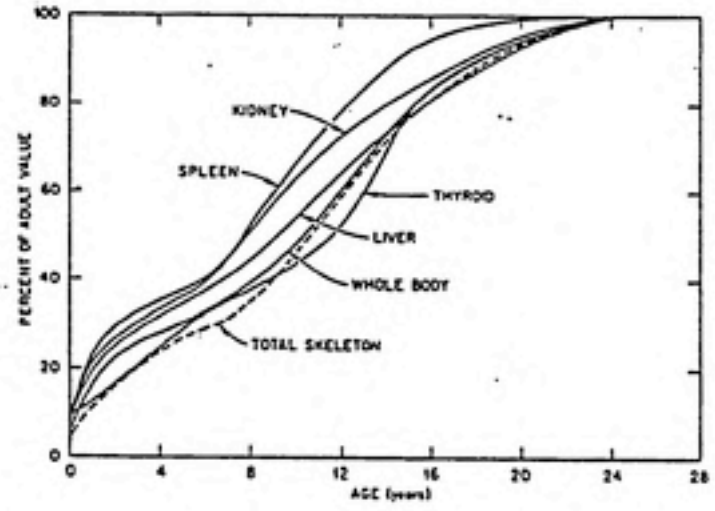

Figure 7 Age Dependence of Organ Masses for the Human

Table 2 provides a list of the fractional rate of organ growth, (1/N)(dN/dt), and the rate of sloughing, S, for each year prior to age 22. Beyond age 22, these rates are constant.

b). Spontaneous Rate of Transition from State 0 to State 1 (k_{0s}):

It is assumed in this analysis that k_{0s} is independent of age. Based on the concept of material balance at equilibrium, the rate of input must be equal to the rate of output for state 0. This relationship, shown in Figure 3, may be formulated as follows:

$$M_s N_{0E} + k^R_1 N_{1E} = (k_{ds} + k_{0s}) N_0 \quad (40)$$

$$\text{Therefore, } k_{0s} = (M_s - k_{ds}) + k^R_1 (N_{1E}/N_{0E}) \quad (41)$$

To maintain organ homeostasis in adults, the background rates of mitosis and cell killing are approximately equal (i.e. $M_s = k_{ds}$). Therefore, the value for k_{0s} is 0.2 day^{-1}.

The spontaneous rate of transition from state 0 to state 1, k_{0s}, is an input for state 1. A cell in state 1 will undergo one of the following three fates: (1) it undergoes further transition to state 2 with a rate of k_{1s}; (2) it is removed by background cell killing with a rate of k_{ds}; or (3) it is repaired and goes back to state 0 at a rate of k^R_1. Due to the relatively large value of k^R_1, the actual rate of transition from state 0 to state 1 is significantly offset by cell repair. Therefore, the fraction of k_{0s} that contributes to transitions is equal to the sum of k_s and k_{1s} divided by the sum of k_s, k_{1s}, and k^R_1. The effective portion of k_{0s}, referred to as $(k_{0s})_{eff}$, is the product of k_{0s} and the fraction of transitions (from state 0 to state 1) which avoid repairing the cells in state 1 back to state 0. This yields :

Table 2 Age-Dependent Values for the Fractional Rate of Organ Growth (1/N)(dN/dt) and the Rate of Sloughing (S) per year

Age	(1/N) (dN/dt)	S
0	0.5	14.45
1	0.35	14.05
2	0.2	12.05
3	0.12	11.5
4	0.08	8.43
5	0.07	7.23
6	0.085	6.67
7	0.09	6.32
8	0.095	6.02
9	0.1	5.06
10	0.11	4.60
11	0.11	4.36
12	0.1	4.08
13	0.095	3.78
14	0.085	3.51
15	0.07	3.24
16	0.05	3.16
17	0.04	2.98
18	0.03	2.81
19	0.03	2.72
20	0.03	2.66
21	0.03	2.58

$$(k_{0s})_{eff} = \left(\frac{k_{ds} + k_{1s}}{k_{ds} + k_{1s} + k^{R}_{1}}\right) k_{0s} \qquad (42)$$

$$= 0.00638 \ (day^{-1})$$

$$= 0.23 \ (year^{-1})$$

In fact, k_0 is a function of dose rate. However, the radiation component is relatively small compared to the background rate. It is assumed that k_0 is not significantly affected by radiation and is independent of age in this study. The constant value of 0.23 (yr^{-1}) derived above is applied to each age.

c). Spontaneous Rate of Transition from State 1 to State 2 (k_{1s}):

As with k_{0s}, k_{1s} is estimated at equilibrium with D equal to zero. This yields :

$$k_{1s} N_{1E} + M_s (1-P_4) N_{3E} = M_s P_4 N_{3E} + k_{ds} N_{3E} \qquad (43)$$

$$\text{Therefore, } k_{1s} = [\, M_s (2P_4-1) + k_{ds} \,] (N_{3E}/N_{1E}) \qquad (44)$$

P_4 is a constant representing the probability per cellular division that a cell in state 3 will undergo transition to state 4. Its value equals 5×10^{-4}, which was determined by Crawford-Brown and Hofmann (C-B90) using the data of Han et al (Han84). N_{3E} times P_4 is the fraction of cells in state 3 undergoing transition to state 4 during mitosis, while the fraction of cells remaining in state 3 will be equal to N_{3E} times $(1-P_4)$. It is assumed here that $M_s = k_{ds}$. The value of k_{1s} is obtained as follows :

$$k_{1s} = 2 P_4 M_s (N_{3E}/N_{1E}) \qquad (45)$$

$$= 1.67 \times 10^{-7} \ (day^{-1})$$

$$= 0.00006 \ (yr^{-1})$$

d). Spontaneous Rate of Transition from State 3 to State 4 (k_{3s}):

The transition from state 3 to state 4 is a division-related fixation, which is proportional to the mitotic rate with a constant P_4.

$$k_{3s} = M_s P_4 \qquad (46)$$
$$= M_s \, 5 \times 10^{-4}$$

e). Spontaneous Rate of Transition from State 4 to State 5 (k_{4s}):

From in-vitro studies, a lifetime probability of spontaneous promotion is determined to be approximately 0.1 (C-B90). This value has been shown to be consistent with limited in-vivo data. Assuming a mean life expectancy of 73 years in the U.S. and a 20-year latency period of developing a lung cancer, the time interval for promotion (neglecting the initiation period) to occur is about 53 years. Therefore,

$$\int_0^{53} k_{4s} \, dt = 0.1 \qquad (47)$$

$$k_{4s} = 2 \times 10^{-3}$$

3.2.2. Radiation Induced Rates

The value of k_{1R} was determined from in-vitro experiments (Roo90), and equals 4×10^{-5} mrad^{-1}. The rate of mitosis is stimulated by cell killing due to exposure to radiation, and the rate of radiation induced mitosis (M_R) is assumed to equal the rate of cell

killing caused by radiation to maintain the lung mass. The value of k_{dR} is taken here to be 1.67×10^{-5} mrad^{-1}.

The parameter $k_{4R}(\dot{D})$ is a radiation induced rate related to contact inhibition removal within the cellular community during mitosis. This depends on a specific number of dead cells surrounding a cell in state 4. As discussed earlier, the total number of cells contiguous to a epithelial cell is six, and at least four of these six cells must be dead to stimulate the transition toward state 5. Assuming binomial distribution, therefore,

$$k_{4R}(\dot{D}) = M(\dot{D}) \sum_{i=4}^{x=6} \frac{x!\ (f)^i\ (1-f)^{x-i}}{(x-i)!\ \ i!} \qquad (48)$$

Here, f is the fraction of dead cells in the tissue surrounding a cell in state 4. It is assumed that cells, except those being killed, are in a dividing state. These surviving cells are removed from the organ by lysis at rate constant R (C-B90). Therefore, f is given by the following relationship :

$$f = \frac{k_d(\dot{D})}{k_d(\dot{D}) + R} \qquad (49)$$

Where R is the rate of removal set equal to 1 day^{-1} to be consistent with the rate of mitosis in heavily damaged organs (C-B91 in press).

A summary of parameter values used in state-vector model of this study is provided in Table 3.

Table 3 Summary of Parameter Values Employed in State-Vector Model

PARAMETER	VALUE	
k_{1R}	4×10^{-5}	$mrad^{-1}$
k_{dR}	1.67×10^{-5}	$mrad^{-1}$
k^R_1	0.13	hr^{-1}
k_0	0.23	yr^{-1}
k_{1s}	0.0061	yr^{-1}
k_{4s}	0.002	yr^{-1}
N_{OE}	0.94	
N_{1E}	0.06	
N_{3E}	0.001	
P_4	5×10^{-4}	
R	1	day^{-1}

IV. RESULTS

The influences of different amounts of ETS on the working level (WL) concentrations of radon progeny and the unattached fractions of RaA (f_a) under various initial particle concentrations (N) are presented in Table 4. The initial particle concentrations refer to the concentrations present before the introduction of ETS.

It is noted that there is a general tendency of increasing working level concentration and decreasing unattached fraction of RaA with greater amounts of ETS. In addition, the presence of ETS only slightly raises the working level concentration, with a maximum increase of a factor of two, but significantly reduces the unattached fraction of RaA by three orders of magnitude which is the largest difference identified. Comparing 2 packs of cigarettes versus smoke free for an initial particle concentration of 10^3 cm^{-3}, the ratio of the WL concentration is equal to 2 (i.e. $3.78 \times 10^{-3}/1.89 \times 10^{-3}$), while the ratio of the RaA unattached fraction increases to 1.45×10^3 (i.e. 0.63/0.0044). Since the dose per inhaled atom is significantly higher for unattached progeny than for those attached, the effects of ETS are more significant when the initial aerosol concentration is as low as 10^3 or 10^4 cm^{-3}.

Table 4 A List of the WL Concentrations of Radon Progeny and the RaA Unattached Fractions under Each Set of Exposure Conditions in the Home

N (particles/c.c.)	Amount smoked (packs/day)	WL	f_a
10^3	0	1.89×10^{-3}	0.63
	1/2	3.73×10^{-3}	0.0172
	1	3.76×10^{-3}	0.0087
	2	3.78×10^{-3}	0.0044
10^4	0	3.29×10^{-3}	0.15
	1/2	3.74×10^{-3}	0.0158
	1	3.77×10^{-3}	0.0084
	2	3.78×10^{-3}	0.0043
10^5	0	3.73×10^{-3}	0.017
	1/2	3.76×10^{-3}	0.0088
	1	3.78×10^{-3}	0.006
	2	3.78×10^{-3}	0.0035
10^6	0	3.79×10^{-3}	0.0018
	1/2	3.79×10^{-3}	0.0016
	1	3.79×10^{-3}	0.0015
	2	3.81×10^{-3}	0.0013

The calculation of annual doses for different ages with different amounts of smoke in the environment are shown in tables 5 to 8 under each set of initial aerosol concentrations.

From the results shown in Tables 5 to 8, the addition of ETS tends to lower the doses of radon progeny to the lung, and an increased amount of smoke in the environment results in a lower dose. This implies that when the initial concentration is so high that almost all the progeny have been attached to particles, the contribution of aerosol particles from ETS has a minimal effect on the calculated progeny doses. In addition, the curve of age-variant doses reveals that the subgroup most sensitive to radon progeny exposure would be children in the ages between 5 and 10.

It is interesting that the doses with ETS present are slightly higher for $N_i = 10^4$ cm^{-3} than those corresponding doses for $N_i = 10^3$ cm^{-3} regardless of age and amounts of cigarette smoke. The similar relationship remains for the case of comparing the doses when N_i raises from 10^5 up to 10^6 cm^{-3}. But, for the case of comparing the doses for $N_i = 10^4$ and 10^5 cm^{-3}, a decreasing tendency of annual doses is found with higher density of initial aerosols present. This fluctuating change of annual doses with different initial aerosol concentrations is the result of many competing factors. Due to the complicated process of dose calculation, it is difficult to pinpoint out a specific factor responsible for this change. Instead of comparing the doses among different values of N_i, however, a comparison concerning the relative change of annual doses with and without ETS present for each initial aerosol concentration may provide an indirect explanation.

The value of RaA unattached fraction (f_a) for $N_i = 10^3$ cm^{-3} without ETS present is approximately four times of that for $N_i = 10^4$ cm^{-3} without ETS present (i.e. 0.63 versus 0.15). The presence of ETS, which will release an amount of particles equal to a magnitude of five orders per cm^3 into the ambient air, reduces the f_a down to approximately the same level for both $N_i = 10^3$ and 10^4 cm^{-3}. For all ages, the addition of ETS equal to 1/2 pack of cigarettes per day lowers the doses by a factor of four for $N_i = 10^3$ cm^{-3} and by a factor of only 2.5 for $N_i = 10^4$ cm^{-3}. Therefore, the higher doses with ETS present for $N_i = 10^4$ compared to 10^3 cm^{-3} may result from the ETS particles that have more significant effect on reducing the RaA unattached fraction for $N_i = 10^3$ cm^{-3} than that for $N_i = 10^4$ cm^{-3}.

The final sensitivity analysis for life-time relative risk of lung cancer (i, e. the possibility of lung cancer with ETS present compared to that without ETS present) is displayed in Table 9.

If the initial aerosol concentration in the home is less than 10^4 cm^{-3}, the addition of ETS equal to less than 1 pack of cigarettes per day may lower the risk of lung cancer. A general trend indicates that the relative risk of lung cancer increases as the initial concentration goes up and more ETS is added.

Table 5 Annual Irradiation Doses for Different Ages and Various Levels of ETS Present with Initial Aerosol Particles Equal to 10^3 cm^{-3}

Age (yrs)	Annual Doses (mrad/year), when Ni=10^3			
	Amount Smoked (packs)			
	0	1/2	1	2
0	280	70	65	65
2	250	63	58	58
5	320	80	75	75
10	340	85	79	79
22	150	38	35	35

Table 6 Annual Irradiation Doses for Different Ages and Various Levels of ETS Present with Initial Aerosol Particles Equal to 10^4 cm^{-3}

Age (yrs)	Annual Doses (mrad/year), when Ni=10^4			
	Amount Smoked (packs)			
	0	1/2	1	2
0	220	84	80	80
2	200	77	73	73
5	250	96	91	91
10	270	102	96	96
22	120	46	44	44

Table 7 Annual Irradiation Doses for Different Ages and Various Levels of ETS Present with Initial Aerosol Particles Equal to 10^5 cm^{-3}

Age (yrs)	Annual Doses (mrad/year), when Ni=105 Amount Smoked (packs)			
	0	1/2	1	2
0	77	61	61	61
2	70	56	56	56
5	88	70	70	70
10	95	76	76	76
22	42	34	34	34

Table 8 Annual Irradiation Doses for Different Ages and Various Levels of ETS Present with Initial Aerosol Particles Equal to 10^5 cm^{-3}

Age (yrs)	Annual Doses (mrad/year), when Ni=106 Amount Smoked (packs)			
	0	1/2	1	2
0	66	66	66	66
2	60	60	60	60
5	75	75	75	75
10	81	81	81	81
22	36	36	36	36

Table 9 Life-time Relative Risks of Lung Cancer under Each Set of Exposure Conditions in the Home

Initial Aerosol Concentration (particles/cm3)	RR ETS/without ETS		
	1/2 packs of cigarettes of ETS	1 pack of cigarettes of ETS	2 packs of cigarettes of ETS
10^3	0.693	0.766	1.000
10^4	0.801	0.889	1.164
10^5	1.060	1.193	1.560
10^6	1.115	1.255	1.641

V. DISCUSSION:

The analysis in Table 9 implies that estimating the possibility of lung cancer depends on various competing factors. The initial aerosol concentration in the home plays an important role in quantifying the effect of ETS on radon exposure.

For relatively low concentrations of aerosol particles (less than $10^4\,cm^{-3}$), the presence of ETS lowers the unattached fraction of RaA and progeny doses dramatically. This may result in a lower risk of lung cancer than a smoke free environment. Combining the promotional effect of ETS by an increased risk of 2.4 % per pack of cigarettes, the final results indicate a decreased relative risk of 0.766 for an initial particle concentration of $10^3\,cm^{-3}$, and 0.889 for an initial particle concentration of $10^4\,cm^{-3}$. Analogously, the smoke from 1/2 pack of cigarettes will result in a decreased relative risk of 0.693 for an initial particle concentration of $10^3\,cm^{-3}$, and 0.801 for an initial particle concentration of $10^4\,cm^{-3}$.

It is noted that the influence of ETS on radon induced lung cancer is related to, but not limited to, the competition of the initial aerosol concentration and the magnitude of promotional effect of ETS. For low initial aerosol concentrations in the home, the particle density in air has a dominating effect on progeny attachment and will yield a relatively lower risk of lung cancer; however, for high

initial aerosol concentrations, the promotional effect outweighs the reduced radiation dose due to the addition of ETS. This will result in a higher risk of lung cancer.

The results predicted from this study are basically consistent with the results from animal experiments. The NRC report (NRC88) found that respiratory tract tumor incidences

* increase with the unattached fraction of radon progeny.
* decrease if cigarette smoking follows completion of exposure to radon progeny, but has no effect if smoking precedes exposure.
* decrease if animals are exposed to smoking and radon progeny alternately on the same day.

The combined lung cancer relative risk of 1.34 from the meta-analysis of 13 epidemiological studies (NRC86) is much higher than would be expected from comparisons of biological markers of smoke exposure between ETS-exposed people and active smokers. The analysis of urinary levels of cotinine discussed in the NRC report (NRC86) suggested that ETS exposure was roughly equivalent to smoking 0.1 to 0.2 cigarettes per day, which is approximately the range used in the present study (i.e. 0.04 to 0.16 cigarettes per day). The excess lung cancer risk calculated from epidemiological studies (34%) is about 10 times greater than the excess lung cancer risk obtained here using extrapolation from MS smoke data to estimate the cigarette equivalence inhaled by the passive smoker (1.2 to 4.8%). The NRC contended that the effects of ETS cannot be precisely compared on the basis of biological markers due to the different components between ETS and MS smoke. Another explanation from

the opposite viewpoint stated that the observed association from epidemiological studies was misclassification of smokers and ex-smokers as nonsmokers. This discrepancy raises the controversy of the association between ETS and lung cancer remained to be further identified.

The most striking conclusion of this study suggests that the effect of ETS on radon-induced lung cancer can not be simply classified as protective, additive, or synergistic. Whether the combined risk is less than, equal to, or greater than these two separate risks primarily depends on the initial aerosol concentration and the amounts of ETS in the home. Several competing factors influence the effect of ETS on radon progeny, which complicates the mitigation schemes.

For the initial particle concentration of 10^3 or 10^4 cm^{-3} and the amount of smoke equal to less than 1 pack of cigarettes per day, the removal of ETS may not result in the expected lower life-time risk of lung cancer. A higher risk is computed in this study. When the initial particle concentration exceeds 10^5 cm^{-3}, the removal of ETS would reduce the excess relative risk approximately 60% for 2 packs of cigarettes per day, 20 to 25% for 1 pack of cigarettes per day, and 5 to 10% for 1/2 pack of cigarettes per day, respectively

VI. RECOMMENDATIONS FOR FUTURE RESEARCH:

As mentioned in the Introduction, there is sufficient evidence from epidemiological studies of uranium miners and from animal experiments to link lung cancer causally to exposure to radon. There are also voluminous studies relating ETS exposure to lung cancer. But very little research dealing with exposure to radon and ETS simultaneously has been undertaken. It would be desirable to conduct further epidemiological studies of the effects of ETS on radon exposure in the home.

As far as the state-vector model is concerned, several assumptions remain to be proved or modified. (1) Even though the effects of radiation as a function of age are considered in the present study, the calculation of accumulative life-time risk based on an assumption of a constant annual dose during each year is untested. That is, this method of breaking down the lifetime into intervals assumes that the effect of changing the dose rate within a given year is negligible. Thus, a better resolution of time for assessing the life-time exposure is needed. (2) The values of the fractional rate of organ growth and the rate of sloughing for each age which are required for estimating the spontaneous rate of mitosis are very approximate. This arises from the lack of specific data for the lung. (3) The rate constant of transition from the naturally undamaged

state to the first damaged state (k_{0s}) may depend on age. This possibility remains unexplored at this time. (4) In this study, all cells are assumed to be identical and do not differentiate into non-dividing cells. However, the radiation-related rate of mitosis, stimulated by cell killing, is associated with the structural features of the cellular community. Further study should be made on the effect of cellular inhomogeneity on the mitotic rates. Finally, (5) the latency period of lung cancer varies greatly with the age of exposure. In the BEIR III report (NRC80), the assignment of latency period is:

Exposure at age	Latency period (years)
0-15	25
15-24	15-20
> 34	10

The value of background promotional rate, k_{4s}, is obtained by assuming an average latency period of 20 years at each age in this study. This suggests that a more accurate procedure for estimating k_{4s} should incorporate age-dependent changes in the latency period. More input is required to determine the latency period of lung cancer related to the exposed age and the dose rate.

The deposition fraction of progeny in the naso-oro-pharyngo-laryngeal (NOPL) region may be affected by the particles from ETS. This provides information about the initial condition for calculating the deposition fraction in the TB region. A more precise NOPL deposition model is required to identify the effects of ETS on deposition of radon progeny above the TB region.

In addition to the effect on the fraction of progeny atoms attached to aerosol particles, ETS may influence breathing

characteristics, airway diameters, mucociliary functions, and thickness of mucus layers (NRC86). Each of these changes will in turn affect deposition and doses of radon progeny in the lung. A model which estimates the combined effect of these factors has been reported (C-B91 in press), but few experimental results are available to support these predictions.

Even though the results from animal studies suggested that radiation acts as an "initiator" and tobacco smoke acts as a "promoter" in the carcinogenic process (Cha81), a more direct proof from human studies is needed to identify the actual role of ETS in affecting initiation, promotion, and progression of radon-exposed lung cancer.

The rationality of extrapolating from MS smoke to ETS, based on the assumption that carcinogenic potency for both MS smoke and ETS is proportional to the mass of RSP deposited in the TB region, remains to be further tested. Clearly, considerable work needs to be done in developing a proper method to assess dose-response of ETS exposure.

REFERENCES:

Ca69 Carnahan, B. et al 1969. Applied Numerical Methods. John Wiley & Sons, Inc. p. 63

Cha81 Chameaud, J.R., et al. 1981. Contribution of animal experimentation to the interpretation of human epidemiological data. In Radiation Hazard in Mining: Control, Measurement, and Medical Aspects, ed. Gomez, M. New York: Society of Mining Engineers: 222-227

C-B84 Crawford-Brown, D. J. 1984. A united approach to age-dependent metabolic modeling. Health Physics, 46 : 809-832.

C-B87 Crawford-Brown, D. J. 1987. Dosimetry. In Environmental Radon, Cothern, C. R. and Smith, J. E. : 173-213

C-B90 Crawford-Brown, D. J. and Hofmann, W. 1990. A generalized state-vector model for radiation-induced cellular transformation. International Journal of Radiation Biology 1990, Vol 57 No 2 : 407-423.

EPA87 Environmental Protection Agency 1987. Radon Reference Manual, EPA 520/1-87-20, Washington, D.C. : The U.S. Environmental Protection Agency.

EPA90 Environmental protection Agency 1990. Health Effects of Passive Smoking: assessment of lung cancer in adults and respiratory disorders in children.

Ev68 Evans, R. E., 1968. Engineering Guide to the Elementary Behavior of Radon Daughters. Health Physics 38: 1173-1197.

Han84 Han, A. Hill, C. K. and Elkind, M. M. 1984. Repair process and radiation quality in neoplastic transformation of mammalian cells. Radiation Research, 99: 249-261.

Hof79 Hofmann, W. , et al 1979. Dose calculation for the respiratory tract from inhaled natural radioactive nuclides as a function of age. Health Physics 37 : 517-532.

In85 Ingebrethson, B. J. and Sears, S. B. 1985. Particle size distribution measurements of sidestream tobacco smoke, presented at the 39th Tobacco Chemists' Research conference, Montreal, Canada.

Kei60 Keith, C. H. and Derrick, J. C. 1960. Measurement of the particle size distribution and concentration of cigarette smoke by the "conifuge". J. Colloid Sci. 15: 340-356.

Kel60 Kells, L. M. 1960. Elementary Differential Equation. McGraw-Hill, New York. p.48.

Lao90 Lao, K. Q. 1990. Controlling Indoor Radon : measurement, mitigation, and prevention. Van Nostraud Reinhold, New York.

Mc80 McPherson, R.B. 1980. Environmental radon and radon daughter dosimetry in the respiratory tract. Health Physics 39 : 929-936.

NRC80 National Research Council, Committee on the Biological Effects of Ionizing Radiations (BEIR III) 1980. The Effect on Populations of Exposure to Low Levels of Ionizing Radiation. Washington, D.C. : National Academy Press.

NRC86 National Research Council 1986. Environmental Tobacco Smoke : Measuring Exposures and Assessing Health Effects. Washington, D.C. : National Academy Press.

NRC88 National Research Council, Committee on the Biological Effects of Ionizing Radiations (BEIR IV) 1988. Health Risks of Radon and other Internally Deposited Alpha-Emitters. Washington, D.C. : National Academy Press.

NRC90 National Research Council, Committee on the Biological Effects of Ionizing Radiations (BEIR V) 1990. Health Effects of Exposure to Low Levels of Ionizing Radiation. Washington, D.C. : National Academy Press.

NCRP88 National Council on Radiation Protection and Measurements 1988. Measurement of Radon and Radon daughters in Air. Report No. 97. Washington D.C. : National Council on Radiation Protection and Measurements.

Raa69 Raabe, O. G. 1969. Concerning the Interactions that Occur between Radon Decay Products and Aerosols. Health Physics, 17: 177-187.

Roe90 Roe, Francis J. C. 1990. Discussion on ETS and lung cancers. In Environmental Tobacco Smoke: Proceedings of the International Symposium at McGill University 1989, ed. Ecobichon, D. J. and Wu, J. M. pp 128-132.

Roo90 Roots, R. Holley, W. Chatterjee, A. Irizarry, M. and Kraft, G. 1990. The Formation of Strand Breaks in DNA after High-LET Irradiation. International Journal Radiation Biology, 58 : 55-70.

Rud86 Rudnick, S. N. and Maher, E. F. 1986. Surface Deposition of Rn-222 Decay Products with and without Enhanced Air Motion. Health Physics, 51 : 283-293.

Shi90 Shimizu, Y. Kato, H. and Schull, W. J. 1990. Studies of the Mortality of A-Bomb Survivors. 9. Mortality, 1950-1985 : Part 2. Cancer Mortality on the Recently Revised Doses (DS 86). Radiation Research, 121 : 120-141.

Wy67 Wynder, E. L. and Hoffman, D. 1967. Tobacco and Tobacco Smoke: Studies in Experimental Carcinogenesis. Academic Press, New York.

APPENDIX

The five age-dependent annual doses under each set of exposure conditions, shown in Tables 5 to 8, were obtained using Hofmann's computer code. Given these data, a method called spline is used to fit a smooth curve through which the annual dose for each age can be interpolated under each set of exposure conditions.

Spline provides an approach to approximating a continuous and differentiable function on the interval [a,b] in a piecewise fashion (Ca69). Let the base points be $a = x_0 < x_1 < ..... < x_{n-1} < x_n = b$, and the corresponding spline functional values be $S_i(x_i)$, $i = 0, 1, 2, ..., n$. A third-degree polynomial is assumed to approximate the true function on each subinterval $[x_i, x_{i+1}]$. This approximating function for each subinterval $S_i(x)$, referred to as the cubic spline function, is given in the form:

$$S_i(x) = a_i + b_i (x - x_i) + c_i (x - x_i)^2 + d_i (x - x_i)^3 \qquad (50)$$

where a_i, b_i, c_i, and d_i are constants need to be determined using the following boundary conditions.

To be continuous, not only the $S_i(x)$ and $S_{i+1}(x)$ but the first and second derivatives for $S_i(x)$ and $S_{i+1}(x)$ must be equal at $x = x_{i+1}$. Therefore,

$$S_i(x_{i+1}) = S_{i+1}(x_{i+1}) \qquad (51)$$

$$S_i'(x_{i+1}) = S_{i+1}'(x_{i+1}) \qquad (52)$$

$$S_i''(x_{i+1}) = S_{i+1}''(x_{i+1}) \qquad (53)$$

$$i = 1, 2, 3, \ldots\ldots n$$

Inserting $x = x_i$ into equation (50) yields:

$$S_i(x_i) = a_i \qquad (54)$$

Also, inserting $x = x_{i+1}$ into $S_{i+1}(x)$ yields:

$$S_{i+1}(x_{i+1}) = a_{i+1} \qquad (55)$$

The values of a_i, b_i, c_i, and d_i can be solved through application of the method of Gaussian back elimination and matrix manipulations for equations (51) to (55). The detailed calculation refers to the "Applied Numerical Methods" by Carnahan, et al (Ca69).

In the present case, ages 0 to 22 are the interval of concern in which the base points referred to as x_0, x_1, x_2, x_3, and x_4 are equal to 0, 2, 5, 10, and 22, respectively. Four separate cubic spline functions are formulated to fit a continuous curve among each set of five given annual doses. The complicated operation of these numerical calculations is handled by computer software. Tables 10 to 13 display the annual doses for each age obtained by fitting the spline functions under each set of exposure conditions. These age-dose curves are basically consistent with the pattern shown in a paper by Hofmann et al. (Hof79).

Table 10 Interpolation of Doses Shown in Table 5 Using the Spline Functions

Age (yrs)	Annual Doses (mrad/yr), when $N_i = 10^3$			
	Amount Smoked (packs)			
	0	1/2	1	2
0	280	70	65	65
1	258.4	64.9	59.9	59.9
2	250	63	58	58
3	263.8	66.4	61.4	61.4
4	291.4	73.1	68.1	68.1
5	320	80	75	75
6	339.4	84.7	79.6	79.6
7	349.2	87.1	81.8	81.8
8	351.2	87.6	82.0	82.0
9	347.5	86.8	81.0	81.0
10	340	85	79	79
11	330.4	82.7	76.6	76.6
12	319.2	80.8	73.9	73.9
13	306.6	76.8	70.9	70.9
14	292.5	73.4	67.5	67.5
15	277.3	69.6	64.0	64.0
16	261.1	65.6	60.2	60.2
17	243.9	61.4	56.3	56.3
18	226.0	56.9	52.2	52.2
19	207.5	52.3	48.0	48.0
20	188.6	47.6	43.7	43.7
21	169.4	42.8	39.4	39.4
22	150	38	35	35

Table 11 Interpolation of Doses Shown in Table 6 Using the Spline Functions

Age (yrs)	Annual Doses (mrad/yr), when $N_i = 10^4$			
	Amount Smoked (packs)			
	0	1/2	1	2
0	220	84	80	80
1	205.4	78.8	74.6	74.6
2	200	77	73	73
3	209.9	80.9	76.6	76.6
4	229.4	88.3	83.7	83.7
5	250	96	91	91
6	264.6	101.3	95.9	95.9
7	272.7	104.0	98.4	98.4
8	275.6	104.8	98.9	98.9
9	274.2	103.9	98.0	98.0
10	270	102	96	96
11	263.8	99.4	93.4	93.4
12	255.9	96.3	90.4	90.4
13	246.6	92.7	87.0	87.0
14	235.9	88.6	83.1	83.1
15	224.0	84.1	79.0	79.0
16	211.1	79.3	74.6	74.6
17	197.3	74.2	69.9	69.9
18	182.7	68.9	64.9	64.9
19	167.6	63.3	59.9	59.9
20	152.0	57.6	54.6	54.6
21	136.1	51.8	49.3	49.3
22	120	46	44	44

Table 12 Interpolation of Doses Shown in Table 7 Using the Spline Functions

Age (yrs)	Annual Doses (mrad/yr), when $N_i = 10^5$			
	Amount Smoked (packs)			
	0	1/2	1	2
0	77	61	61	61
1	71.9	57.3	57.3	57.3
2	70	56	56	56
3	73.4	58.9	58.9	58.9
4	80.6	64.3	64.3	64.3
5	88	70	70	70
6	93.2	74.1	74.1	74.1
7	96.1	76.4	76.4	76.4
8	97.1	77.3	77.3	77.3
9	96.5	77.1	77.1	77.1
10	95	76	76	76
11	92.8	74.4	74.4	74.4
12	90.0	72.2	72.2	72.2
13	86.6	69.6	69.6	69.6
14	82.9	66.7	66.7	66.7
15	78.7	63.4	63.4	63.4
16	74.1	59.7	59.7	59.7
17	69.1	55.9	55.9	55.9
18	64.1	51.7	51.7	51.7
19	58.7	47.5	47.5	47.5
20	53.2	43.0	43.0	43.0
21	47.7	38.5	38.5	38.5
22	42	34	34	34

Table 13 Interpolation of Doses Shown in Table 8 Using the Spline Functions

Age (yrs)	Annual Doses (mrad/yr), when $N_i = 10^6$			
	Amount Smoked (packs)			
	0	1/2	1	2
0	66	66	66	66
1	61.6	61.6	61.6	61.6
2	60	60	60	60
3	63.0	63.0	63.0	63.0
4	68.8	68.8	68.8	68.8
5	75	75	75	75
6	79.4	79.4	79.4	79.4
7	81.8	81.8	81.8	81.8
8	82.7	82.7	82.7	82.7
9	82.3	82.3	82.3	82.3
10	81	81	81	81
11	79.1	79.1	79.1	79.1
12	76.8	76.8	76.8	76.8
13	74.0	74.0	74.0	74.0
14	70.8	70.8	70.8	70.8
15	67.2	67.2	67.2	67.2
16	63.3	63.3	63.3	63.3
17	59.2	59.2	59.2	59.2
18	54.8	54.8	54.8	54.8
19	50.3	50.3	50.3	50.3
20	45.6	45.6	45.6	45.6
21	40.8	40.8	40.8	40.8
22	36	36	36	36